



AN EXPERIMENTAL STUDY ON DAMAGE-RESISTANT REINFORCED CONCRETE SHEAR WALLS

Tolou Kian, Mohammad Javad¹ and Cruz Noguez, Carlos^{1,2}

¹ University of Alberta, Canada

² cruznogu@ualberta.ca (corresponding author email)

Abstract: Today, reinforced concrete (RC) structures are designed to deform in a ductile manner when resisting strong ground motions. However, when structures deform beyond their elastic limits, sustaining permanent drift ratios and suffering concrete damage, which can lead to costly retrofitting or even demolition and reconstruction plans becomes unavoidable. In this regard, an experimental study was undertaken to explore the seismic performance of three types damage-resistant RC shear walls. The study included the cyclic testing of three innovative shear walls detailed with innovative reinforcements and fibre reinforced cementitious composite (FRCC). The reinforcing system of each specimen consisted of steel rebars and a type of self-centering reinforcement such as shape memory alloy (SMA) bars, glass fibre reinforced polymer (GFRP) bars or high-strength steel strands. Test results showed that innovative shear walls detailed with high-performance materials had reduced residual drift ratios and mitigated concrete damage in comparison to a conventionally designed and constructed control shear wall. In addition, each innovative shear wall exhibited more than 3% of inelastic rotation, which was both code compliant and comparable to that of the control specimen.

1 INTRODUCTION

Earthquake-resisting reinforced concrete (RC) elements including RC shear walls can effectively support structural systems against seismic loads. However, these elements are susceptible to sustaining permanent displacements and concrete damage when undergoing nonlinear deformations. These disadvantages stem from the plastic elongation of steel rebars after yielding and the brittle response of concrete in tension. Given the fact that conventional materials and methods of construction have their own intrinsic limitations, today innovative materials and construction techniques are becoming more appealing in structural engineering.

Post-tensioning is a technique used to improve the seismic performance of shear walls. (Holden et al 2003) showed a precast concrete shear walls detailed with post-tensioned tendons illustrates substantial self-centering and mitigated damage under cyclic loads. However, the energy dissipation capacity of the wall was limited due to the lack of continuous bonded reinforcement through the joint of the precast wall. Another technique is to detail the boundaries of RC shear walls with bars made of shape memory alloy (SMA). (Abdulridha and Palermo 2013) tested a concrete shear wall which was reinforced with both steel and SMA bars. The experiment showed that the innovative shear wall had improved self-centering with respect to a purely steel reinforced control wall although the wall suffered severe damage along its SMA reinforced regions. Another method, which was studied by (Mohamed et al. 2013), was to incorporate GFRP bars in the construction of concrete shear walls. The study consisted of testing three concrete shear walls

reinforced with glass fibre reinforced polymer (GFRP) bars. According to test results, purely GFRP reinforced walls had substantial self-centering with satisfactory levels of deformability and strength. However, the walls had limited levels energy dissipation due to the linear behaviour of their GFRP reinforcement.

Given the fact that each of the previous studies was successful in improving the performance of RC shear walls in certain areas, this exploratory study was defined to improve the overall performance of a conventional RC shear wall through the reduction of permanent deformations and concrete damage without compromising the ductility and energy dissipating properties of the wall.

2 EXPERIMENTAL PROGRAM

This paper studies damage-resistance in four slender shear walls built with identical geometries and comparable reinforcement schemes but different materials and details. Two indicators were used to identify damage in the specimens – permanent residual drift ratio and concrete damage i.e. cracking and spalling. To that end, three of the shear walls were reinforced with conventional steel bars and a type of self-centering reinforcement either SMA bars, GFRP bars, or high-strength steel strands. The specimens were also cast with fibre reinforced cementitious composites (FRCC) for concrete damage reduction. Casting innovative shear walls with FRCC also guaranteed the adequate initial stiffness of the specimens. However, as experiments progressed and the innovative walls started to crack, their responses became less influenced by the fibre reinforcement used in their construction and more by their longitudinal reinforcement.

2.1 Material Properties

The materials used in this experimental study consisted of cementitious and reinforcing materials. The cementitious materials included normal concrete, steel fibre reinforced concrete (SFRC) and engineered cementitious composite (ECC). The fibres used in ECC were 12 mm long and made of PVA (poly vinyl alcohol). According to Choi and Lee (2015) the PVA fibres used in ECC have a minimum aspect ratio of 300, and a minimum tensile strength of 1000 MPa. The fibres used in SFRC were 50 mm long, hooked-end and made of steel. According to the manufacturer the steel fibres had an aspect ratio of 55, and a tensile strength of 1200 MPa. In terms of composition, ECC did not contain coarse aggregates, while concrete and SFRC contained coarse aggregates with a maximum dimension 10 mm. The water to cement ratio of ECC was 0.57, almost twice as that in concrete and SFRC. The compressive strengths of the cementitious materials used in the construction of shear wall specimens, control specimen (steel-RC wall), GFRP-ECC wall, PT-SFRC wall, and SMA-SFRC wall, were 48 MPa, 38 MPa, 62 MPa, and 51 MPa respectively.

In tension, ECC forms uniform cracking. For this reason, the tensile properties of the material were identified through the test of ECC prisms under direct tension. On the other hand, the tensile behaviour of SFRC is more influenced by crack opening rather than uniform cracking. Therefore, the tensile response of SFRC was evaluated through the test of notched SFRC beams under four-point loading as per (fib 2013). Figures 1(a) and 1(b) show the results of three direct tension tests performed on three ECC prisms corresponding to GFRP-ECC wall and two four-point loading tests performed two SFRC beams corresponding to PT-SFRC and SMA-SFRC walls.

Figure 1(a) shows the tensile stress-strain relationship of each of the three ECC prisms. According to test results, the ECC material used in the construction of GFRP-ECC wall had an average tensile stress of 3.1 MPa. The tensile strain capacity of the material was about 1% as the ECC material exhibited a plateau after the linear part of its tensile stress-strain relationship. In contrast, the tensile stress-strain relationship of concrete does not contain a plateau as with the propagation of the first crack the material rapidly losses its tensile resistance. Figure 1(b) shows the outcomes of two four-point loading tests in terms of applied load versus crack mouth opening displacement (CMOD). In SFRC beam specimens, fibres bridging cracks

transferred tensile stresses. As a result, the beams were able to maintain their load bearing capacities after cracking. However, a concrete, beam specimen loses its load bearing capacity with the formation and propagation of cracks. Then, using equilibrium calculations, flexural tensile stress-CMOD relationship of each SFRC beam was derived. According to (fib 2013), flexural tensile stress in a notched beam under four-point loading at CMODs of 0.5 mm and 2.5 mm can be used to evaluate the post-cracking behaviour of the SFRC material of which the specimen was made. The SFRC beam corresponding to SMA-SFRC wall had flexural tensile stress values of 3.5 MPa and 3.88 MPa at CMODs of 0.5 mm and 2.5 mm. These stress values were 5.55 MPa and 4.75 MPa respectively for the SFRC beams corresponding to PPT-SFRC wall.

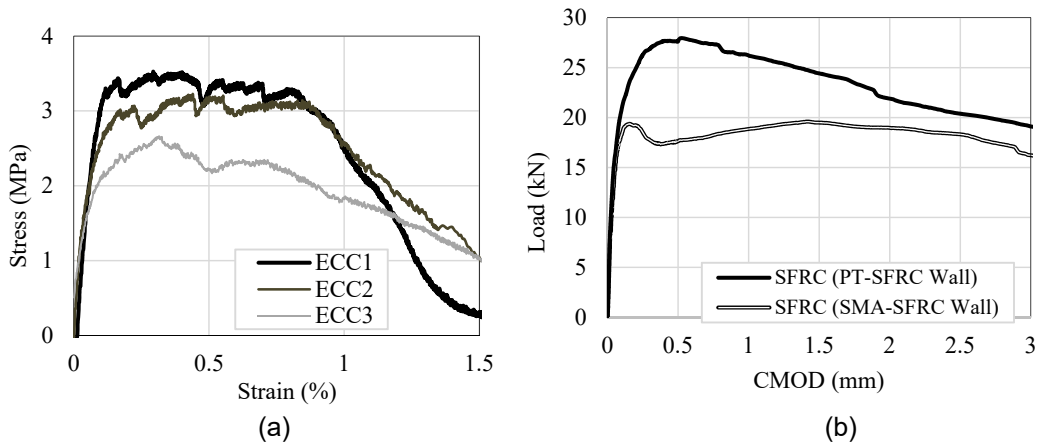


Figure 1: Tensile properties of FRCC materials (a) ECC (b) SFRC

The different types of reinforcement used in this study as well as the nominal diameter and cross-sectional area of each are as follows: 10M (11.3 mm, 100 mm²) steel rebar, #5 (15.9 mm, 199 mm²) GFRP bars, #4 (12.7 mm, 127 mm²) NiTi bars and 0.5-inch (12.7 mm, 98.7 mm²) high-strength steel strands. Figure 2 shows the tensile stress-strain relationship of each type of reinforcement calculated based on its nominal geometries. As shown in Figure 2, GFRP bars and high-strength steel strands behave linearly in a broader range of tensile stresses in comparison to mild steel bars. This property of GFRP bars and high-strength steel strands can be used to improve the self-centering of structural elements. On the other hand, NiTi bars exhibit a super-elastic property and which enables them to recover applied strain of up to 6%. This property of NiTi bars can be used towards the promotion of self-centering in RC elements as well.

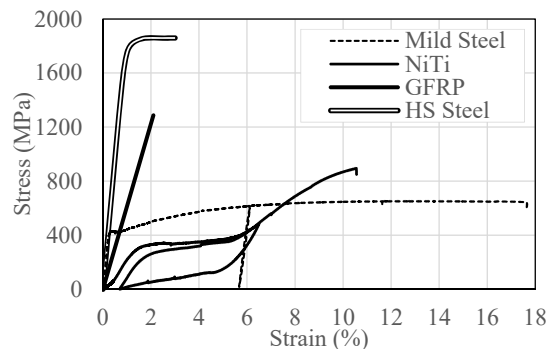


Figure 2: Stress-strain relationships of reinforcing materials

Mechanical properties of #5 GFRP bars were provided by the manufacturer. The bars had an ultimate strain of 2.1%, an ultimate stress of 1150 MPa and a stiffness of 62.6 GPa. #5 GFRP bars were sand coated. For

this reason, the bars had an effective diameter of 17.3 mm and an effective cross-sectional area of 235 mm², which were larger than the nominal properties of the bars. However, the stress resistance properties of the GFRP bars were corresponding to their nominal area since the coating of the bars does not participate in the resistance of tensile stresses. Mechanical properties of 0.5" high-strength steel strands were provided by the manufacturer as well. 0.5" high-strength steel strands had a yield stress of 1670 MPa, an ultimate strength of 1860 MPa and a stiffness of 195 GPa.

In case of #4 NiTi bars, a #4 NiTi coupon specimen was tested according to (ASTM F2516-14 2014). The NiTi bar had an elastic modulus of 27.4 GPa, an upper plateau strength (UPS) of 330 MPa, and a lower plateau strength (LPS) of 120 MPa. The tensile strain capacity of the NiTi bar was equal to 10.5%, corresponding to a stress capacity of 890 MPa. The material properties of mild steel bars were determined according to (ASTM A370-14 2014). The 10M steel rebars used in the construction of CW and SMA-SFRC wall had an elastic modulus of 174 GPa, a yield stress of 421 MPa and an ultimate strength of 634 MPa. The forgoing properties for the 10M rebars used in the construction of GFRP-ECC and PPT-SFRC walls were 185 GPa 415 MPa and 626 MPa respectively.

2.2 Test Specimens

Each specimen was comprised of a wall panel supported by a foundation and cap-beam. To restrain the translational and rotational displacements at the bases of wall panels, the foundation of each specimen was anchored to the strong floor of the laboratory. Each cap-beam was anchored to the loading unit which was used to apply in-plane displacement reversals in accordance to (ATC 24 1992) to the specimens. The out-of-plane displacement component at the top point of each specimen was restrained since it was desired to study the in-plane response of the walls. The response of each specimen was measured using eight cable transducers, six LVDTs as well as a clinometer mounted on the surfaces of the specimen (Figure 3(a)) while a digital image correlation (DIC) system was capturing displacements on the opposite side of the specimen (Figure 3(b)).

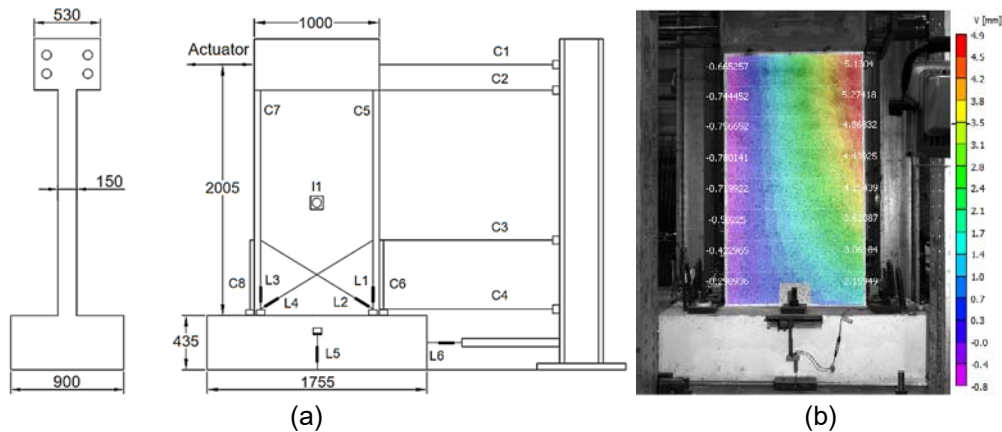


Figure 3: A test specimen (a) dimensions and instrumentation (b) DIC output example

The total number of specimens was four. The specimens were designed in accordance to the seismic provisions for reinforced concrete structures in North America, (CSA A23.3-14 2014) and (ACI 318-14 2014). In the meanwhile, (CSA S806-12 2012) and (CPCI 2007) were used in the design of the innovative walls as well. The first shear wall was a conventional steel reinforced concrete shear wall, which was considered as the control specimen of the study and termed the control wall or CW (Figure 4(a)).

Innovative shear walls were termed GFRP-ECC, SMA-SFRC and PT-SFRC based on the self-centering reinforcement and the type of the cementitious material used in their construction. The rationale of the design of the innovative shear walls was to increase the self-centering of the control wall with three types

self-centering reinforcement while the reinforcement layout of the specimen is preserved to the extent possible. As shown in Figure 4, each innovative specimen was detailed with a type of self-centering reinforcement in addition to steel reinforcement, which was primarily used to ensure the energy dissipation and ductility of the specimen. The innovative specimens were also cast with FRCC to have improved damage resilience. However, as soon as the shear walls had formed flexural cracks, their responses were controlled by their longitudinal reinforcement rather than the cementitious composite they were cast with. In particular, just one innovative wall was cast with ECC in this study due to some restraints in providing the material. Therefore, the other two innovative walls were cast with SFRC.

In case of GFRP-ECC and PPT-SFRC walls, shown in Figures 4(b)-(c), boundaries were reinforced with mild steel, while self-centering reinforcements, which had much lower strain capacities than mild steel, were placed within the webs of the shear walls. In this way, the specimens were provided with improved self-centering properties as well as substantial levels of ductility and energy dissipation. As shown in Figure 4(d), NiTi bars were placed along the boundaries of SMA-SFRC wall. Also, due to the high price of NiTi bars, only up to a height of 550 mm of the boundaries of SMA-SFRC wall were reinforced with SMA and the sections above and below the SMA reinforced regions were reinforced with 15M steel rebars to limit nonlinear rebar elongations at the boundaries to the NiTi bars.

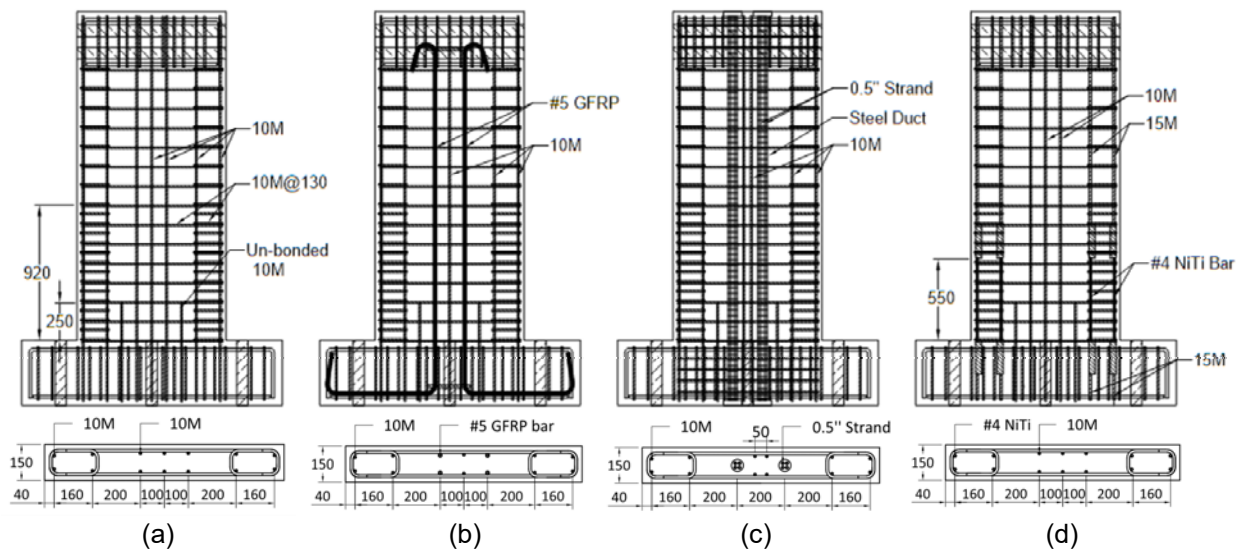


Figure 4: Reinforcement layout of (a) CW (b) GFRP-ECC (c) PT-SFRC (d) SMA-SFRC

In addition, since the elastic limits of GFRP and high-strength steel were notably higher than that of mild steel, a shear wall specimen detailed with GFRP bars or high-strength steel strands and with similar lateral load strength to that of the control wall was bound to have inadequate ratio of self-centering reinforcement to exhibit a meaningful self-centering characteristic. For this reason, having a comparable reinforcement layout to that of the control wall with maximum self-centering was considered as the design objective of GFRP-ECC and PT-SFRC walls. As a result, it was decided that #5 GFRP bars be used in GFRP-ECC wall and each post-tensioned tendon in PT-SFRC wall consist of four 0.5" high-strength steel strands.

On the other hand, in case of SMA-SFRC wall, it was possible to increase the self-centering of the control wall while maintaining the lateral strength of the wall. This was because #4 NiTi and 10M steel bars required comparable amounts of tensile force to yield. For this reason, #4 NiTi bars were selected to be used in SMA-SFRC wall.

2.3 Test Results

2.3.1 Damage Resilience

Figure 5 displays the distribution of vertical strains measured by the DIC system on the surface of each wall panel at a drift ratio of 3.2%. As can be seen in Figure 5, the distributions of vertical strains can clearly show the cracking patterns of shear walls. According to Figure 5, GFRP-ECC sustained only few cracks, SMA-SFRC and PPT-SFRC walls suffered moderate cracking and spalling, and the control wall sustained more cracking and cover spalling than other specimens. On the other hand, the control wall had less crack opening as the wall formed more cracks than other specimens. At 3.25% drift, the maximum crack opening in SMA-SFRC, PPT-SFRC, GFRP-ECC and CW walls was 26 mm, 24 mm, 18 mm and 14 mm respectively.

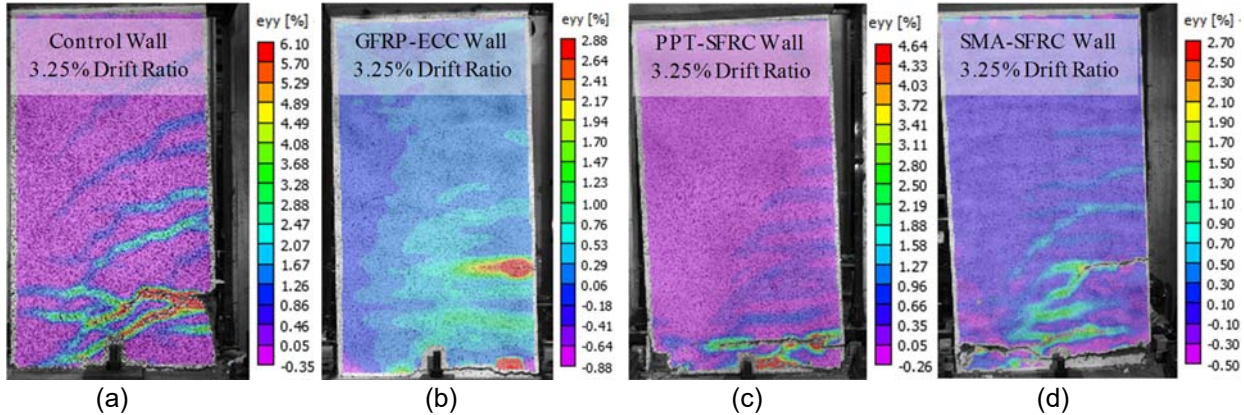


Figure 5: Vertical strains at 3.25% drift ratio (a) CW (b) GFRP-ECC (c) PT-SFRC (d) SMA-SFRC

Rupturing of longitudinal steel rebars was the damage after which specimens underwent strength degradation and consequently failure. For GFRP-ECC, PPT-SFRC and CW walls the first steel rebar rupture occurred at drift ratios of 2.72%, 2.75% and 3.25%. However, in case of SMA-SFRC wall, it was at 5.0% drift when the first row of longitudinal steel reinforcement in the web of the shear wall ruptured.

2.3.2 Hysteresis Response

The hysteretic response of each shear wall and the equivalent energy elastic-plastic (EEEP) idealization of its backbone curve according to (Park 1988) is shown in Figure 6. According to the figure, each specimen exhibited a symmetric, stable response with significant amounts of ductility and energy dissipation. In addition, innovative specimens featured reduced residual drifts in comparison to the control wall as well.

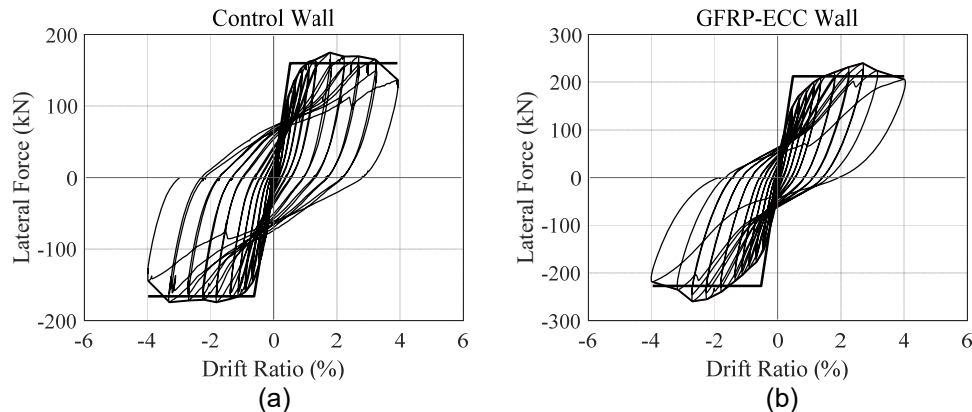


Figure 6: Hysteretic response of specimens (a) CW (b) GFRP-ECC (c) PT-SFRC (d) SMA-SFRC

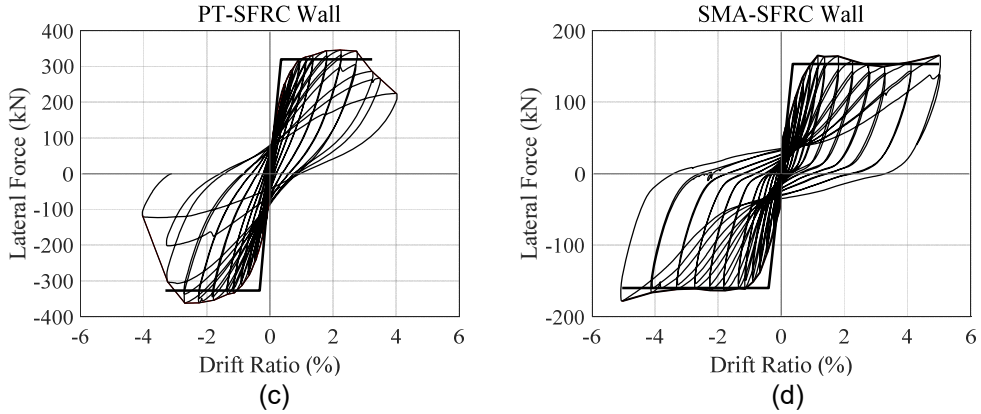


Figure 6: Continued

Figure 7 illustrates the residual drift ratio of each specimen in the first repetition of each level of lateral displacement. As can be seen in Figure 7, residual drift ratios of specimens increased with the progress of experiments. Also, innovative shear walls showed generally higher self-centering in comparison to the control wall as the walls sustained less permanent deformations and recovered more of their lateral drift ratios upon unloading. For instance, after unloading from a drift ratio of 3.25%, CW had a permanent drift of 2.2%, while it was 1.6%, 1.4%, and 0.8% for GFRP-ECC, SMA-SFRC, and PT-SFRC walls respectively, corresponding to 27%, 36% and 65% reduction in comparison to the residual drift of the control wall. After unloading from -3.25% drift, the residual drift ratios of SMA-SFRC and GFRP-ECC walls were about -1.7%, while it was -1.4% for PT-SFRC wall. This was associated with 24% and 27% reduction in the residual drift ratios of SMA-SFRC and GFRP-ECC walls, and 37% reduction in that of PT-SFRC wall in comparison to -2.3%, the residual drift ratio of the control wall.

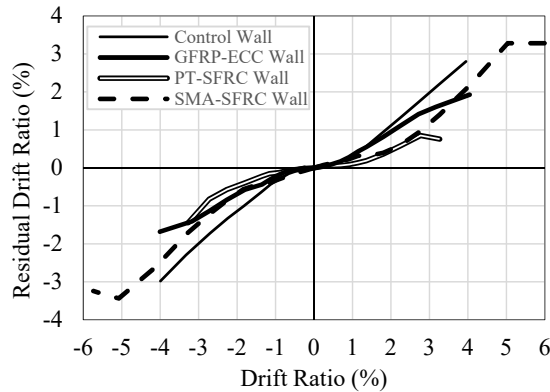


Figure 7: Residual drift ratios of specimens

2.3.3 Rotational Deformation

Figure 8 illustrates the distribution of rotations along the height of each shear wall. The rotation values at different heights of walls were obtained based on Equation 1.

$$[1] \theta(h) = \frac{V_T(h) - V_C(h)}{l}$$

In Equation 1, V_T and V_C are vertical elongations measured by the DIC system on the tensile and compressive sides of shear walls at a height of h . The parameter l in Equation 1 is also the distance between the two elongation measurements.

As can be seen in Figure 8, at the beginning of testing (0.1% drift ratio), rotation distributions along the heights of specimens were almost linear since no major cracking or excessive reinforcement elongation due to the yielding had occurred. As experiments progressed, the most of rotational deformations took place within the plastic hinge lengths of the specimens – approximately a height of $0.5l_w$ from the base of the shear walls according to (Park and Paulay 1975) with l_w being the length of the walls. As can be seen from Figure 8, SMA-SFRC wall reached, a rotational capacity of 0.062 rad, the highest among the specimens, while the capacities of GFEP-ECC, CW and PPT-SFRC walls were 0.042 rad, 0.038 rad and 0.034 rad respectively. The yield rotation of CW based on EEEP method was 0.005 rad. Yield rotation for each of GFRP-ECC, SMA-SFRC and PT-SFRC walls was 0.006 rad, 0.005 rad and 0.002 rad respectively.

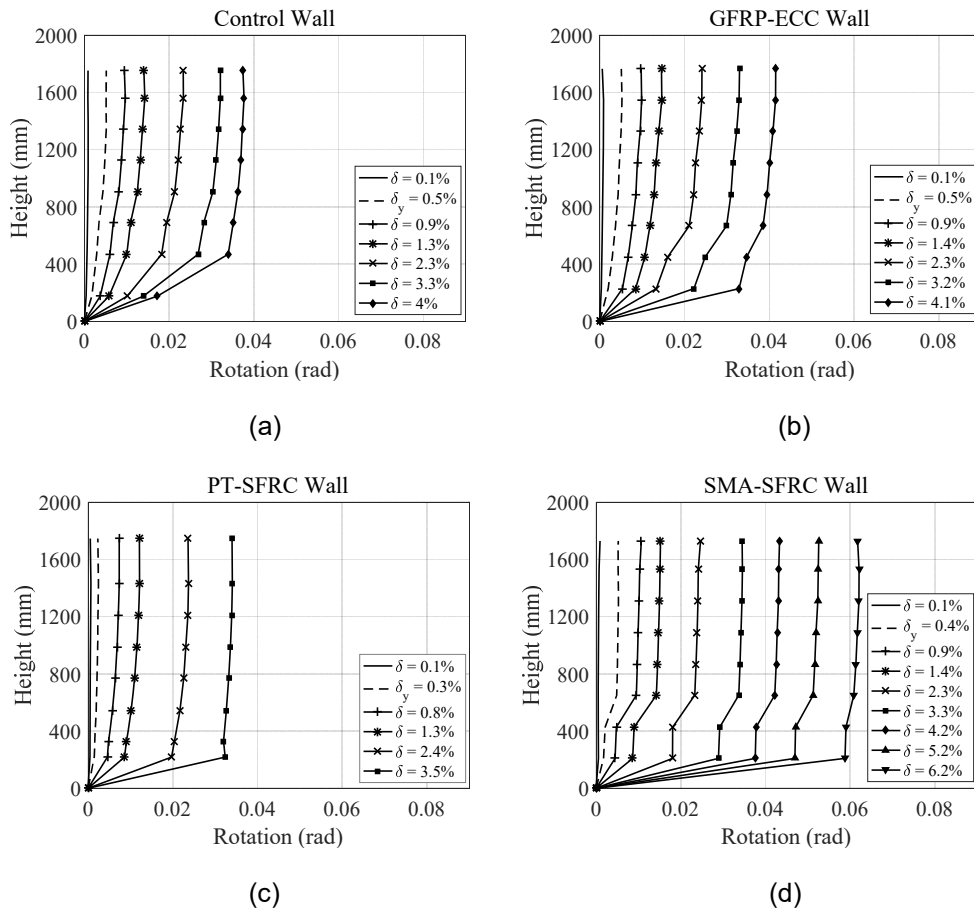


Figure 8: Distribution of rotation along the heights of the specimens (a) CW (b) GFRP-ECC (c) PT-SFR (d) SMA-SFRC

Figure 9 illustrates the inelastic rotations that each shear wall specimen underwent during testing. As can be seen from Figure 9, the SMA-SFRC wall was able to reach an inelastic rotation capacity of 0.056 rad, the highest among the specimens. The maximum inelastic rotation of GFRP-ECC wall was 0.041 rad, while it was about 0.032 rad for CW and PPT-SFRC walls. It is worthwhile to mention that the inelastic rotation capacities of all the specimens were higher than 0.025 rad, the CSA 23.3-14 upper limit on inelastic rotation capacity controlled by tension steel strain in ductile RC shear walls.

As can be seen in Figure 8, most of rotational displacements were concentrated at sections close to the bases of shear walls, where most of concrete cracking and reinforcement yielding took place. In order to, compare the distribution of rotation along the heights of shear walls, the rotation distributions of walls at 2.3% drift ratio is shown in Figure 10.

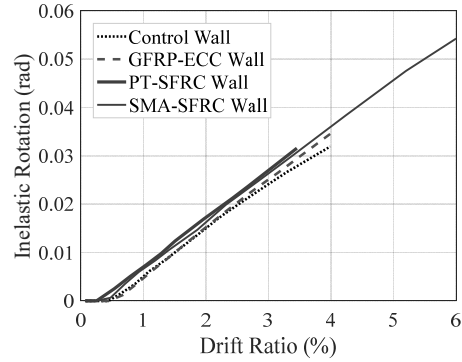


Figure 9: Inelastic rotations of specimens during testing

As can be seen in the Figure 10, although rotation at the top of each wall panel was about 0.024 rad, CW and GFRP-ECC walls underwent less concentrated rotational deformations in their bases in comparison to SMA-SFRC and PT-SFRC walls. This is also in line with the maximum crack opening of the specimens. In fact, since SMA-SFRC and PT-SFRC experienced more crack opening than CW and GFRP-ECC walls, they consequently experienced more concentrated rotational deformations at their cracking locations within their plastic hinge regions.

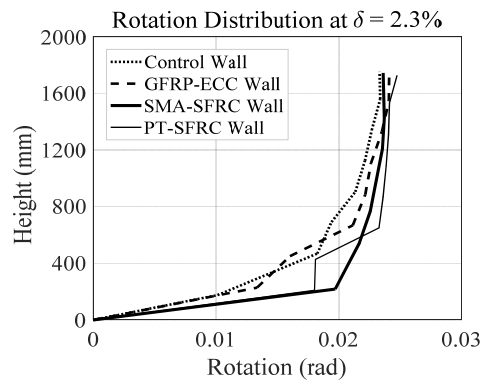


Figure 10: Rotation distribution along the heights of specimens at 2.3% drift ratio

3 CONCLUSIONS

The following conclusions were drawn from this experimental study performed on three innovative shear walls cast with fibre reinforced cementitious composite and reinforced with steel and self-centering reinforcement.

1. Innovative shear walls exhibited more pinched hysteretic responses due to their smaller residual drift ratios in comparison to the control wall.
2. Innovative shear walls sustained mitigated damage in terms of cracking and covers spalling in comparison to the control shear wall. On the other hand, the control wall had smaller amounts of maximum crack opening as the specimen formed more cracks than the innovative walls.
3. The inelastic rotation capacities of all innovative wall were greater than 0.03 rad.
4. SMA-SFRC wall, which was detailed with SMA in its boundaries, exhibited a greater ultimate drift ratio with respect to other specimens due to the elimination of outmost rebar rupturing.

5. The placement of GFRP bars and high-strength steel strands in the webs of the GFRP-ECC and PT-SFRC walls protected the self-centering reinforcements from high tensile strain demands and failure.

References

- Abdulridha, A. and Palermo, D. 2014. Response of a hybrid-SMA reinforced concrete shear wall. *Tenth U.S. National Conference on Earthquake Engineering: Frontiers of Earthquake Engineering*, Anchorage, Alaska, USA.
- ACI (American Concrete Institute). 2014. *Building code requirements for structural concrete*. ACI 318-14, Farmington Hills, MI, USA.
- ATC (Applied Technology Council). 1992. *Guidelines for Cyclic Seismic Testing of Components of Steel Structures*. Redwood City, California, USA.
- ASTM. 2014. *Standard test methods and definitions for mechanical testing of steel products*. ASTM A370-14, West Conshohocken, PA.
- ASTM. 2014. *Standard test method for tension testing of nickel-titanium superelastic materials*. ASTM F2516-14, West Conshohocken, PA.
- Canadian Standards Association (CSA). 2012. *Design and construction of building structures with fibre-reinforced polymers*. CSA S806-12, Mississauga, Ontario, Canada.
- Canadian Standards Association (CSA). 2014. *Design of concrete structures*. CSA A23.3-14, Mississauga, Ontario, Canada.
- Canadian Precast/Prestressed Concrete Institute (CPCI). 2007. *CPCI Design 4*, Ottawa, Ontario, Canada.
- Choi, J. and Lee, B. Y. 2015. Bonding properties of basalt fiber and strength reduction according to fiber orientation. *Materials*, **8**: 6719-6727.
- Fédération Internationale du Béton (fib). 2013. *fib Model Code for Concrete Structures 2010*. Lausanne, Switzerland.
- Holden, T., Restrepo, J. and Mander, J. B. 2003. Seismic performance of precast reinforced and prestressed concrete walls. *Journal of Structural Engineering*, **129**(3): 286-296.
- Mohamed, N., Sabry Farghaly, A., Benmokrane, B. and Neale, K. W. 2014. Experimental investigation of concrete shear walls reinforced with glass fiber-reinforced bars under lateral cyclic loading. *Journal of Composite Construction*, **18**(3): 1-10.
- Park, R. 1988. Ductility evaluation from laboratory and analytical testing. *Ninth World Conference on Earthquake Engineering*, Tokyo-Kyoto, Japan: 605-616.
- Park R. and Paulay T. 1975. *Reinforced Concrete Structures*. John Wiley & Sons Inc., Hoboken, NJ, USA.